

Generating coherent state of entangled spins

Hongyi Yu, Yu Luo, and Wang Yao*

Department of Physics and Center of Theoretical and Computational Physics, The University of Hong Kong, Hong Kong, China

(Dated: October 26, 2018)

A coherent state of many spins contains quantum entanglement which increases with a decrease in the collective spin value. We present a scheme to engineer this class of pure state based on incoherent spin pumping with a few collective raising/lowering operators. In a pumping scenario aimed for maximum entanglement, the steady-state of N pumped spin qubits realizes the ideal resource for the $1 \rightarrow \frac{N}{2}$ quantum telecloning. We show how the scheme can be implemented in a realistic system of atomic spin qubits in optical lattice. Error analysis show that high fidelity state engineering is possible for $N \sim O(100)$ spins in the presence of decoherence. The scheme can also prepare a resource state for the secret sharing protocol and for the construction of large scale Affleck-Kennedy-Lieb-Tasaki (AKLT) state.

PACS numbers: 03.67.Bg,42.50.Dv,37.10.Jk,37.30.+i

I. INTRODUCTION

Coherent state in quantum mechanics usually refers to a specific type of quantum states with minimum uncertainty. It was first discovered in the context of oscillator field and has found wide applications in quantum optics [1–4]. A quantum harmonic oscillator in coherent state most closely resembles the behavior of a classical oscillator. The notion was later generalized to spin systems [5–8]. In an ensemble of N spin- I particles, the term spin coherent state (or atomic coherent state) is used to denote the states where the collective spin $\hat{\mathbf{J}} \equiv \sum_n \hat{\mathbf{I}}_n$ has the minimum uncertainty [8]. Such states can be easily identified in the basis $|J, \mu, \vec{\lambda}\rangle$ which are eigenstates of \hat{J}^2 and \hat{J}_z with eigenvalues $J(J+1)$ and μ respectively, and $\vec{\lambda}$ denotes additional quantum numbers to provide a complete set of labels. The collective spin J gets every value from NI down to 0 (or $\frac{1}{2}$) in integer steps, and for each collective spin value J , the magnetic quantum number $\mu = -J, -J+1, \dots, J$. One can easily show that the minimum uncertainty relation $\langle(\Delta\hat{J}_x)^2\rangle\langle(\Delta\hat{J}_y)^2\rangle = \frac{1}{4}\langle\hat{J}_z\rangle^2$ is satisfied for all extremal states $|J, \mu = -J, \vec{\lambda}\rangle$ in this basis. Hence these states and their rotations generated by $\hat{\mathbf{J}}$ are the spin coherent states (SCS) [8]. Interestingly, two contrary characters coexist on these states: the most classical collective spin behavior; and the fundamentally non-classical phenomenon of quantum entanglement. For every $J < NI$, there is a degenerate set of $|J, -J, \vec{\lambda}\rangle$ with identical collective properties and distinct entanglements where the number of unentangled spins is upper bounded by $\frac{J}{I}$ [9].

Preparation of SCS has been possible only in limited cases. The $J = NI$ SCS, nondegenerate and unentangled, is obtained when all spins are fully polarized. Most experimental studies of spin squeezing start on this state. Schemes were also proposed to populate mixed state of singlets ($J = 0$ SCS) by collective pumping [10], and to select out singlet by projective measurement in a scattering model [11]. Engineering a pure-state SCS of an arbitrary J value is a challenge but of

multi-fold significance. It is the sufficient condition for initialization into a decoherence free subsystem for robust quantum computation under strong collective decoherence [12]. SCS of $J \ll NI$ are resources of large scale entanglement with potential uses in one-way quantum computation [13, 14]. The ability to access a SCS of entangled spins also opens up a new realm for the study of the interrelation between collective spin behaviors and quantum correlations in a spin ensemble [15, 16].

In this paper, we propose control schemes for engineering pure-state SCS of an arbitrarily specified collective spin value in a general spin ensemble. The schemes are based on incoherent spin pumping of the N target spins and a set of ancilla spins by a few (e.g. three) collective raising/lowering operators. The desired pure state is obtained with an N -independent probability by a single projective measurement on the steady state of the pumping, and the success rate approaches 100% with $O(10)$ cycles of pump plus measure. In a simplified pumping scenario aimed for maximum entanglement, the steady state of N pumped spin qubits (without measurement projection) realizes the ideal resource for $1 \rightarrow \frac{N}{2}$ optimal quantum telecloning [17]. We show how the scheme can be implemented in the realistic system of atomic spin qubits trapped in optical lattice, where the collective spin pumping is realized by Stokes or anti-Stokes light scattering. Error analyses show that high fidelity state engineering is possible for up to $N \sim O(100)$ atomic spin qubits in the presence of control errors and decoherence. This is a concrete example of using simple and robust irreversible dynamics to prepare a desired complicated quantum state [18–23]. The scheme can also prepare resource state for the secret sharing protocol [24], and for efficient construction of large scale AKLT state with applications in one-way quantum computation [25–27].

II. GENERAL SCHEME

Key to the state engineering approach by irreversible dynamics is to design the dissipative controls under which the system saturates to the desired state vectors. We utilize here the spin pumping process which drives a spin system towards a mixture of all singlets connected to the initial state by the

*wangyao@hkuc.hku.hk

pumping operators [10]. If a target spin ensemble is in singlet with a spin- J ancilla, its collective spin value must also equal to J . With a proper constraint from conserved quantum numbers, the singlet can be unique from which the desired pure-state SCS of the target spins can be obtained.

The target spins are divided into two subgroups with collective spin $\hat{\mathbf{j}}_A$ and $\hat{\mathbf{j}}_B$ respectively, and the collective spin of $2J$ spin- $\frac{1}{2}$ ancillas is denoted by $\hat{\mathbf{j}}_\beta$. When an inhomogeneous collective operator of the form $\hat{J}_i^+ = c_A \hat{j}_A^+ + c_B \hat{j}_B^+ + c_\beta \hat{j}_\beta^+$ acts on a SCS, the final state can be generally written as

$$\hat{J}_i^+ |J_T, -J_T, \vec{\lambda}\rangle = \sum_{\Delta, \vec{\lambda}'} \chi_{J_T, \vec{\lambda}}^{J_T + \Delta, \vec{\lambda}'} |J_T + \Delta, -J_T + 1, \vec{\lambda}'\rangle. \quad (1)$$

where the first two quantum numbers in the kets denote the total spin and the z -component of $\hat{\mathbf{J}}_T = \hat{\mathbf{j}}_A + \hat{\mathbf{j}}_B + \hat{\mathbf{j}}_\beta$ respectively. Calculation of the coefficients χ is straightforward by expanding the collective spin states in terms of common eigenstates of $\hat{J}_A^z, \hat{J}_B^z, \hat{J}_\beta^z$ and \hat{J}_T^z . We find that only the $\Delta = 0, \pm 1$ transitions are allowed [10], and the ratio between transition rates $\Delta = \pm 1$ is

$$\left| \chi_{J_T+1, \vec{\lambda}}^{J_T, \vec{\lambda}'} \right|^2 = (J_T + 1)(2J_T + 1) \left| \chi_{J_T, \vec{\lambda}'}^{J_T+1, \vec{\lambda}} \right|^2. \quad (2)$$

Consider the incoherent strong pump by \hat{J}_T^- which results in a mixture of SCS of $\hat{\mathbf{J}}_T$, and the weak pump by the inhomogeneous operator \hat{J}_i^+ which then causes transitions between these SCS with the effective rate $\propto |\chi|^2$ and the selection rule $\Delta = 0, \pm 1$. From Eq. (2), we can see the $\Delta = -1$ transition is much faster than the $\Delta = 1$ one between any such pair of states. Thus, the pump will saturate the target and ancilla spins to singlets of $\hat{\mathbf{J}}_T$ where J_T is minimized. With the target and ancilla spins initialized on the fully polarized state, the quantum numbers $j_A = N_A I$, $j_B = N_B I$ and $j_\beta = J$ are all conserved by the pump operators. Only one singlet exists under this constraint:

$$|S_{AB\beta}\rangle \equiv \sum_{\mu=-J}^J (-)^{J-\mu} |J, \mu, j_A, j_B\rangle_{AB} \otimes |J, -\mu\rangle_\beta, \quad (3)$$

where $|J, \mu, j_A, j_B\rangle_{AB}$ denotes eigenstates of $(\hat{\mathbf{j}}_A + \hat{\mathbf{j}}_B)^2$ and $\hat{j}_A^z + \hat{j}_B^z$ with eigenvalues $J(J+1)$ and μ respectively.

Fig. 1(a) presents a simulation of the spin pump using the Lindblad master equation $\dot{\rho} = -\frac{1}{2} \sum_{m=0}^2 (\hat{L}_m^\dagger \hat{L}_m \rho + \rho \hat{L}_m^\dagger \hat{L}_m - 2\hat{L}_m \rho \hat{L}_m^\dagger)$, where $\hat{L}_0 \equiv \sqrt{\Lambda_h} \hat{J}_T^-$ and $\hat{L}_m \equiv \sqrt{\Lambda_i} \hat{J}_m^+$ for $m = 1, 2$. Here we have chosen the inhomogeneous raising operators

$$\hat{J}_1^+ = e^{\frac{2}{3}\pi i} \hat{j}_A^+ + e^{\frac{4}{3}\pi i} \hat{j}_B^+ + \hat{j}_\beta^+, \quad \hat{J}_2^+ = e^{\frac{4}{3}\pi i} \hat{j}_A^+ + e^{\frac{8}{3}\pi i} \hat{j}_B^+ + \hat{j}_\beta^+,$$

while other choices of coefficients $c_{A,B,\beta}$ lead to similar results. For the simulated example, we set the spin pump rates $\Lambda_h/\Lambda_i = 5000$, and $j_A = j_B = j_\beta = 5$. After a pump time $t_p = 0.2\Lambda_i^{-1}$, $|S_{AB\beta}\rangle$ is occupied by a population $P(0) \sim 20\%$. For general values of j_A, j_B and j_β , we require

$$\Lambda_h \langle \hat{J}_T^+ \hat{J}_T^- \rangle \gg \Lambda_i \langle \hat{J}_i^- \hat{J}_i^+ \rangle, \quad (4)$$

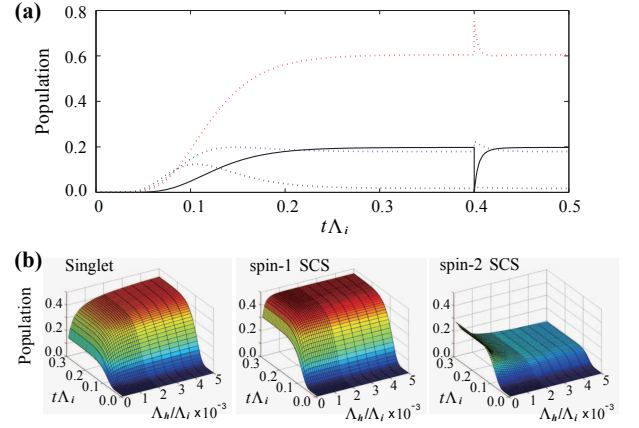


FIG. 1: (a) Simulation of spin pump and repump by the collective operators \hat{J}_T^-, \hat{J}_1^+ and \hat{J}_2^+ (see text). The target and the ancilla spins are in the fully polarized state at $t = 0$. Solid curve: population on the singlet $|S_{AB\beta}\rangle$. Dotted curves: populations in the subspace of $J = 1$ (red), $J = 2$ (blue), and $J = 3$ (black) respectively. We assume the singlet is projected out at $t = 0.4\Lambda_i^{-1}$, and hence the curve after is the repump dynamics. (b) Simulation of the simplified scheme for engineering the telecloning resource for $N = 40$ qubits. The populations on the singlet $|0, 0, \frac{N}{4}, \frac{N}{4}\rangle$, the spin-1 SCS $|1, -1, \frac{N}{4}, \frac{N}{4}\rangle$, and the spin-2 SCS $|2, -2, \frac{N}{4}, \frac{N}{4}\rangle$ are shown as functions of time using various pumping rates.

which ensures the lowering operator \hat{J}_T^- to be applied much more frequently than the raising operator \hat{J}_i^+ . The largest possible value of $\langle \hat{J}_i^- \hat{J}_i^+ \rangle$ is $\sim (j_A + j_B + j_\beta)^2$ while the smallest possible value of $\langle \hat{J}_T^+ \hat{J}_T^- \rangle$ is ~ 1 . Thus $\Lambda_h/\Lambda_i \gg (j_A + j_B + j_\beta)^2$ is sufficient to ensure the condition in (4). The steady-state population on $|S_{AB\beta}\rangle$ is given by $[\sum_k g(k)]^{-1} = 20\%$ where $g(k) \equiv (2k+1) \prod_{i=0}^{k-1} (2i^2 + 3i + 1)^{-1}$ [10]. The timescale to reach steady-state is $\sim (j_A + j_B + j_\beta)^{-1} \Lambda_i^{-1}$. The singlet can be selected out by projective measurement of \hat{J}_T^z or \hat{J}_T^x . If the measurement outcome is not singlet, the spins can be repumped to the steady state in a much shorter timescale $\sim (j_A + j_B + j_\beta)^{-2} \Lambda_i^{-1}$ [Fig. 1(a)]. The probability of NOT obtaining $|S_{AB\beta}\rangle$ is reduced to 0.1% after 30 cycles of measure plus repump.

From the singlet $|S_{AB\beta}\rangle$, further pumping by the target spin operator $\hat{j}_A^- + \hat{j}_B^-$ bring the target spins to the desired SCS $|J, \mu = -J, j_A = N_A I, j_B = N_B I\rangle$. Here the collective spin value J of the target spins is controlled by the number of the ancilla spins involved. Different choices of N_A and N_B realize distinct pure SCS of the same collective spin value, which are fully symmetric under permutation of spins within subgroup A (or B). A and B can also be initialized with any $j_A < N_A I$ and $j_B < N_B I$ by applying the scheme first to the subgroups. Concatenation of the scheme can therefore realize pure SCS with more general permutation symmetries.

SCS of the smallest collective spin values are most desirable as a resource of entanglement. We consider the $J = 0$ scenario of the above scheme (i.e. no ancilla spins) which uses two pump operators: the homogeneous $\hat{j}_A^- + \hat{j}_B^-$ and the inhomogeneous $\hat{j}_A^+ - \hat{j}_B^+$, where A and B each contain $\frac{N}{2}$ tar-

get spins. For $\Lambda_h/\Lambda_i \gg N^2$, we find the steady state of the pumping $\rho = \sum_J P(J)|J, -J, \frac{N}{2}I, \frac{N}{2}I\rangle\langle J, -J, \frac{N}{2}I, \frac{N}{2}I|$ where $P(J) = (2J^2 + 3J + 1)P(J + 1)$. This steady state is reached with a pump time $t_p \approx \frac{3 + \ln NI}{2NI} \Lambda_i^{-1}$ by our numerical estimation, and is largely a mixture of the singlet $|0, 0, \frac{N}{2}I, \frac{N}{2}I\rangle$, the spin-1 SCS $|1, -1, \frac{N}{2}I, \frac{N}{2}I\rangle$, and the spin-2 SCS $|2, -2, \frac{N}{2}I, \frac{N}{2}I\rangle$, with some residue population of 0.5% on the spin-3 SCS $|3, -3, \frac{N}{2}I, \frac{N}{2}I\rangle$. These states can be distinguished in a non-demolition way by measuring $\hat{j}_A^z + \hat{j}_B^z$. A single cycle of pump plus measure thus ends up with one of these pure states which all have large scale entanglement. Fig. 1(b) shows simulation of this spin pumping for a cluster of 40 spin qubits.

The singlet $|0, 0, \frac{N}{4}, \frac{N}{4}\rangle$ of N qubits turns out to be the ideal resource for universal optimal quantum teleportation [17]. If Alice holds subgroup A and each of her $\frac{N}{2}$ associates holds a qubit in subgroup B, Alice can transmit identical copies of her unknown state $\cos \frac{\theta}{2}|0\rangle + \sin \frac{\theta}{2}e^{i\phi}|1\rangle$ with a fidelity of $F_0 = \frac{2N+2}{3N}$ to the $\frac{N}{2}$ associates using local operations and classical communications (LOCC) [17]. By a single cycle of pump plus measure, the success rate to obtain this state is $\sim 46\%$, which is a substantial improvement over the existing scheme where the success rate is $\frac{2}{2+N}$ [11]. Most remarkably, all alternative outcomes by our scheme, i.e. $|J, -J, \frac{N}{4}, \frac{N}{4}\rangle$ with a finite but small J , can also be used as quantum teleportation resource under the same LOCC. Following the same procedure of Ref. [17] but replacing $|0, 0, \frac{N}{4}, \frac{N}{4}\rangle$ with $|J, -J, \frac{N}{4}, \frac{N}{4}\rangle$, we obtain the teleportation fidelity which is then a function of θ [Fig. 2(a)], and it reaches the maximum value on the equator of the Bloch sphere.

$$F_J^{\max} = \frac{(3J+4)N^2 + 4(J+1)N - 4J(J+1)(J+2)}{2(2J+3)N^2}$$

Since $F_J^{\max} > F_0$, better teleportation fidelity can be achieved with these finite J SCS in the presence of partial information (i.e. the range of the θ value). For $N \gg J$, the teleportation fidelity averaged over the entire Bloch sphere approaches F_0 [Fig. 2(b)]. Thus, the mixed steady state of the spin pumping can be used as an equally efficient teleportation resource as the ideal singlet.

A major cause of error for the state engineering is local spin decoherence process. If each spin loses its phase coherence with a rate γ , a total leakage of $\sim N\gamma t_p \sim \gamma/\Lambda_i$ out of the desired subspace is accumulated in the entire duration $t_p \sim \frac{1}{N}\Lambda_i^{-1}$ of the state preparation. High fidelity state engineering thus requires: $\gamma \ll \Lambda_i$. This is confirmed by numerical simulation for a cluster of $N = 8$ spin qubits where we have added pure dephasing processes described by Lindblad operators $\sqrt{2\gamma}\hat{I}_n^z$ for all spins [Fig. 3(a-d)]. We also studied the effect of errors from system parameters. For the simulation presented in Fig. 3(e-h), spins are pumped instead by $\hat{\Xi}_A^- + \hat{\Xi}_B^-$ and $\hat{\Xi}_A^+ - \hat{\Xi}_B^+$ where $\hat{\Xi}^\pm \equiv \sum_n (1 + \eta_n)\hat{I}_n^\pm$, η_n being a random error between η and $-\eta$. The figure of merit is reasonably good when the error amplitude $\eta < 10\%$. Moreover, by pumping with the operators $U(\hat{j}_A^- + \hat{j}_B^-)U^\dagger$ and $U(\hat{j}_A^+ - \hat{j}_B^+)U^\dagger$ where $U \equiv \prod_n \exp(i\theta_n \hat{I}_n^z)$, the state $U|J, -J, \frac{N}{2}I, \frac{N}{2}I\rangle$ is obtained instead of $|J, -J, \frac{N}{2}I, \frac{N}{2}I\rangle$.

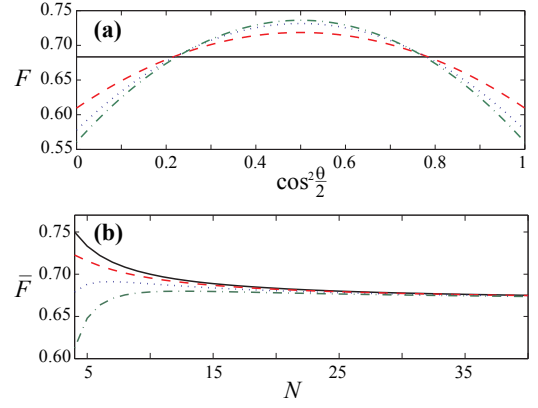


FIG. 2: (a) Fidelity of $1 \rightarrow 20$ teleportation of a state $\cos \frac{\theta}{2}|0\rangle + \sin \frac{\theta}{2}e^{i\phi}|1\rangle$ using the above singlet (solid), spin-1 SCS (dashed), spin-2 SCS (dotted), and the spin-3 SCS $|3, -3, \frac{N}{4}, \frac{N}{4}\rangle$ (dot-dashed) as the resource respectively. (b) The fidelity of $1 \rightarrow \frac{N}{2}$ teleportation (averaged over the Bloch sphere) using the above resource states respectively.

Namely systematic phase errors in the collective pumping operators do not affect the entanglement, and single spin rotations about the z -axis can be deliberately encoded in the pumping.

When A and B each contains 2 qubits, the resultant singlet $|0, 0, 1, 1\rangle$ by our scheme is the 4-qubit AKLT state $P_{23}|S\rangle_{12}|S\rangle_{34}$, where $|S\rangle_{ij}$ stands for the singlet of qubit i and j , and P_{jk} is the projection operator to the triplet subspace for qubit j and k [25]. Its optical analog has been used to demonstrate four-party secret sharing [24], and measurement based single qubit rotation [26]. This state is also an efficient element to construct a large scale AKLT state as schematically illustrated in Fig. 4. Consider two 4-qubit clusters in $P_{23}|S\rangle_{12}|S\rangle_{34}$ and $P_{67}|S\rangle_{56}|S\rangle_{78}$ respectively, by measuring the parity of atom pair $\{4, 5\}$, the spin configuration of this pair will be projected to either the singlet or the triplet subspace [28]. With 75% probability, the measurement outcome is triplet and an 8-qubit AKLT chain $P_{23}P_{45}P_{67}|S\rangle_{12}|S\rangle_{34}|S\rangle_{56}|S\rangle_{78}$ is obtained. The rest 25% probability will give $P_{23}P_{67}|S\rangle_{12}|S\rangle_{36}|S\rangle_{78} \otimes |S\rangle_{45}$ where a 6-qubit AKLT state is obtained. With our scheme as an efficient source of 4-qubit AKLT states, a long AKLT chain can thus be constructed.

III. APPLICATION TO ATOMS IN OPTICAL LATTICE

Here we apply our scheme to cold atoms of a typical Λ -level structure which are trapped in optical lattice. This system has been widely explored in various schemes for quantum information processing. The two lower energy levels are used to represent the spin qubit (Fig. 5(a)). The atoms trapped in an optical lattice can be first initialized to the $|\downarrow\rangle$ state and loaded into a Fabry-Perot cavity (Fig. 5(b)). For simplicity, we assume the optical lattice constants in both directions equal to the wavelength of the cavity mode and all atoms are at the

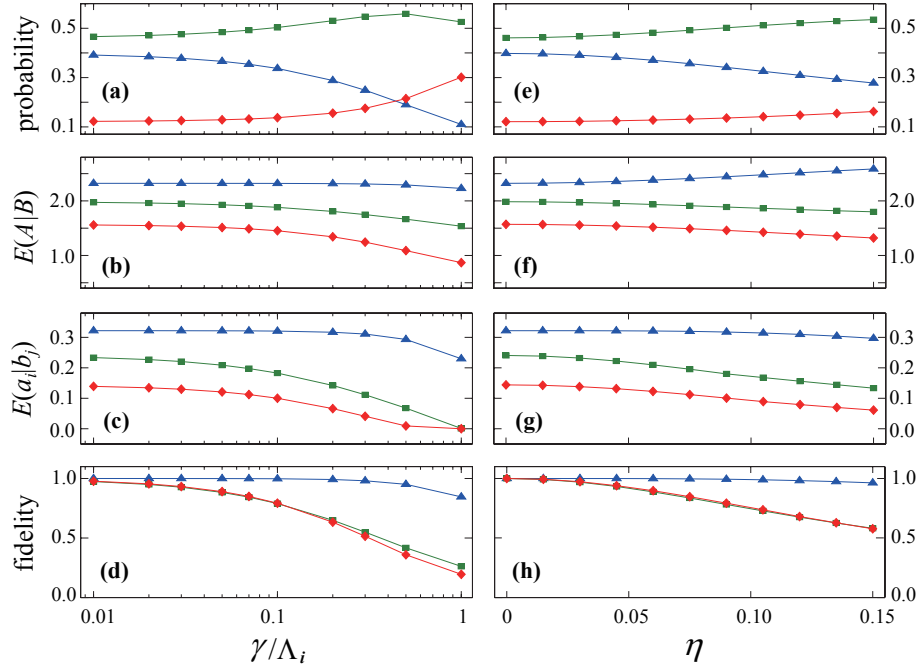


FIG. 3: Merits of state engineering in presence of spin decoherence (a-d) and system parameter errors (e-h) for engineering the telecloning resource for $N = 8$ qubits. $\Lambda_h/\Lambda_i = 100$. (a) and (e): Probability of obtaining singlet (blue triangle), spin-1 SCS (green square) and spin-2 SCS (red diamond) at $t_p = 0.75\Lambda_i^{-1}$. (b) and (f): Bipartite entanglement $E(A|B)$ in the obtained states measured with the logarithmic negativity. (c) and (g): Entanglement between one qubit in A and another in B. (d) and (h): Fidelity of the obtained states with the target states

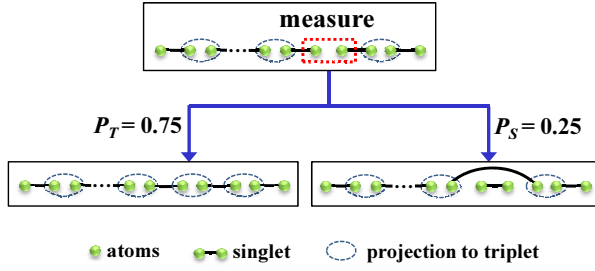


FIG. 4: Increasing the length of a AKLT chain with the resource of 4-qubit-AKLT-state. By measure the parity of the two atoms, the n -qubit AKLT chain either becomes a $(n+4)$ -qubit (lower left) or a $(n+2)$ -qubit AKLT chain (lower right). See text.

peak of the cavity field. Driven by two lasers of frequency $\omega_c \pm \omega_z$ with ω_c being the cavity resonance and ω_z the spin splitting, the cavity-assisted Raman process lowers/raises the spin state. The Raman processes in the large detuning regime ($g^2, \Omega_{\pm}^2 \ll \Delta^2$) can be described by the effective Hamiltonian

$$\hat{H}_{\pm} = \frac{g\Omega_{\pm}}{2\Delta_{\pm}} \hat{J}^{\pm}(\mathbf{k}) \hat{a}_c^{\dagger} + \text{h.c.}, \quad (5)$$

where Ω_{\pm} is the Rabi frequency of the two pumping lasers, g the atom-cavity coupling and Δ_{\pm} the detuning. \hat{a}_c^{\dagger} creates a cavity photon and $\hat{J}^{\pm}(\mathbf{k}) \equiv \sum_j e^{-i\mathbf{k}\cdot\mathbf{r}_j} \hat{\sigma}_j^{\pm}$ realizes various collective spin raising/lowering operations by controlling the

laser wavevector \mathbf{k} . For the setup shown in Fig. 5(b) where the pump lasers are perpendicular to the cavity axis, ‘blue’ laser with $\theta_1 = \frac{\pi}{2}$ realizes the homogeneous operator \hat{J}_T^{-} , and ‘green’ laser with $\cos\theta_2 = \frac{1}{3}$ (or $\frac{2}{3}$) realizes the inhomogeneous collective operator \hat{J}_1^{+} (or \hat{J}_2^{+}) where subgroup A, B and ancilla are represented by blue, red and green spheres respectively.

Projective measurement for selecting out the singlet state can be realized in the same setup. Applying a ‘blue’ and a ‘green’ laser with both $\theta = \frac{\pi}{2}$ and comparable Rabi frequency $\Omega_- \sim \Omega_+$ realizes the homogeneous raising and lowering operators \hat{J}_T^{\pm} on the spin qubits. If the system is in finite J state, then Raman scatterings are allowed and we shall observe continuous cavity photon emission when \hat{J}_T^{+} and \hat{J}_T^{-} pump the spins. When the system is in singlet, Raman scattering is forbidden since both \hat{J}_T^{+} and \hat{J}_T^{-} annihilate the state and there will be no cavity photon emission.

The Raman scattering rate by a single atom is $\Lambda_{h/i} = P\Gamma\Omega_{\pm}^2/\Delta_{\pm}^2$ with Γ being the spontaneous emission rate of atomic excited state in vacuum and P the cavity induced enhancement factor (Purcell factor). Consider the Cs atom ($\frac{\Gamma}{2\pi} = 2.6$ MHz) in a typical Fabry-Perot cavity with mode volume of $10^4 \mu\text{m}^3$ and quality factor 1.7×10^7 , which correspond to $P \approx 80$, $\frac{g}{2\pi} \approx 45$ MHz and cavity decay rate $\frac{\kappa}{2\pi} \approx 20$ MHz [29]. $\Lambda \approx 15$ MHz can then be achieved with $\frac{\Delta}{2\pi} \approx 150$ MHz and $\frac{\Omega}{2\pi} \approx 40$ MHz [30]. The collective Raman scattering rates shall satisfy $\Lambda_i \langle \hat{J}_1^{-} \hat{J}_1^{+} \rangle \ll$

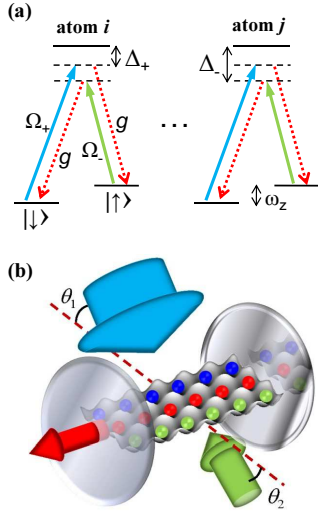


FIG. 5: (a) The level structure of the atoms. Red arrow represents the cavity field, and blue and green arrows denote two laser fields. (b) Collective spin pumping of atoms realized by cavity assisted Raman process. Atoms are trapped in optical lattice and loaded into a Fabry-Perot cavity. The inhomogeneous coefficients are controlled by laser emission angles θ_1 and θ_2 .

$\Lambda_h \langle \hat{J}_T^+ \hat{J}_T^- \rangle < \kappa$ [10], the last inequality is to ensure the emission of cavity photon is spontaneous. For N atoms in cavity, the matrix element $\langle \hat{J}_T^+ \hat{J}_T^- \rangle$ ($\langle \hat{J}_1^- \hat{J}_1^+ \rangle$) is $\sim N$ ($\sim N$) in the neighborhood of the polarized initial state and ~ 1 ($\sim \frac{N^2}{4}$) in the neighborhood of the target singlet state. We can thus use a $\Lambda_h \sim 15$ MHz. Correspondingly, Λ_i shall be ramped down from an initial value of ~ 1 MHz to the steady state value $\sim \frac{1}{N^2}$ MHz along with the spin pumping. Since atom in optical lattice can be of an ultra-slow spin decoherence rate $\frac{\gamma}{2\pi} \sim 1 - 25$ Hz [31], the condition $\gamma \ll \Lambda_i$ can be satisfied for $N \sim O(100)$ qubits.

The authors acknowledge X. D. Xu for helpful comments. The work was supported by the Research Grant Council of Hong Kong under Grant No. 706711P.

-
- [1] W. M. Zhang, D. H. Feng and R. Gilmore, *Rev. Mod. Phys.* **62**, 867 (1990).
- [2] J. R. Glauber, *Phys. Rev. Lett.* **10**, 84 (1963).
- [3] J. R. Glauber, *Phys. Rev.* **130**, 2529 (1963).
- [4] E. C. G. Sudarshan, *Phys. Rev. Lett.* **10**, 277 (1963).
- [5] J. R. Klauder, *J. Math. Phys.* **4**, 1055 (1963).
- [6] A. M. Perelomov, *Commun. Math. Phys.* **26**, 222 (1972).
- [7] R. Gilmore, *Ann. Phys.* **74**, 391 (1972).
- [8] F. T. Arecchi, E. Courtens, R. Gilmore, and H. Thomas, *Phys. Rev. A* **6**, 2211 (1972).
- [9] G. Tóth and M. W. Mitchell, *New J. Phys.* **12**, 053007 (2010).
- [10] W. Yao, *Phys. Rev. B* **83**, 201308 (2011).
- [11] F. Ciccarello, M. Paternostro, S. Bose, D. E. Browne, G. M. Palma, and M. Zarcone, *Phys. Rev. A* **82**, 030302 (2010).
- [12] J. Kempe, D. Bacon, D. A. Lidar, and K. B. Whaley, *Phys. Rev. A* **63**, 042307 (2001).
- [13] D. Gottesman and I. L. Chuang, *Nature* **402**, 390 (1999).
- [14] R. Raussendorf and H. J. Briegel, *Phys. Rev. Lett.* **86**, 5188 (2001).
- [15] A. S. Sørensen and K. Mølmer, *Phys. Rev. Lett.* **86**, 4431 (2001).
- [16] O. Gühne and G. Tóth, *Phys. Rep.* **474**, 1 (2009).
- [17] M. Mura, D. Jonathan, M. B. Plenio, and V. Vedral, *Phys. Rev. A* **59**, 156 (1999).
- [18] S. Diehl, A. Micheli, A. Kantian, B. Kraus, H. P. Buchler, and P. Zoller, *Nat. Phys.* **4**, 878 (2008).
- [19] F. Verstraete, M. M. Wolf, and J. I. Cirac, *Nat. Phys.* **5**, 633 (2009).
- [20] S. Clark, A. Peng, M. Gu, and S. Parkins, *Phys. Rev. Lett.* **91**, 177901 (2003).
- [21] S. Schneider and G. J. Milburn, *Phys. Rev. A* **65**, 042107 (2002).
- [22] J. Cho, S. Bose, and M. S. Kim, *Phys. Rev. Lett.* **106**, 020504 (2011).
- [23] M. J. Kastoryano, F. Reiter, and A. S. Sørensen, *Phys. Rev. Lett.* **106**, 090502 (2011).
- [24] S. Gaertner, C. Kurtsiefer, M. Bourennane, H. Weinfurter, *Phys. Rev. Lett.* **98**, 020503 (2007).
- [25] I. Affleck, T. Kennedy, E. H. Lieb, and H. Tasaki, *Phys. Rev. Lett.* **59**, 799 (1987).
- [26] R. Kaltenbaek, J. Lavoie, B. Zeng, S. D. Bartlett, and K. J. Resch, *Nat. Phys.* **6**, 850 (2010).
- [27] A. S. Darmawan and S. D. Bartlett, *Phys. Rev. A* **82**, 012328 (2010).
- [28] A. M. Rey, V. Gritsev, I. Bloch, E. Demler and M. D. Lukin, *Phys. Rev. Lett.* **99**, 140601 (2007).
- [29] C. J. Hood, T. W. Lynn, A. C. Doherty, A. S. Parkins, and H. J. Kimble, *Science* **287**, 1447 (2000).
- [30] M. Mitsunaga, T. Mukai, K. Watanabe, and T. Mukai, *J. Opt. Soc. Am. B*, **13**, 2696 (1996).
- [31] U. Schnorrberger, J. D. Thompson, S. Trotzky, R. Pugatch, N. Davidson, S. Kuhr, and I. Bloch, *Phys. Rev. Lett.* **103**, 033003 (2009). R. Zhao, Y. O. Dudin, S. D. Jenkins, C. J. Campbell, D. N. Matsukevich, T. A. B. Kennedy, and A. Kuzmich, *Nat. Phys.* **5**, 100 (2008).